

# 1 **Inhibitory effect of eslicarbazepine acetate and S-licarbazepine on** 2 **Na<sub>v</sub>1.5 channels**

3 **Theresa K. Leslie<sup>1</sup>, Lotte Brückner<sup>1</sup>, Sangeeta Chawla<sup>1,2</sup>, William J. Brackenbury<sup>1,2\*</sup>**

4 <sup>1</sup>Department of Biology, University of York, Heslington, York, YO10 5DD, UK

5 <sup>2</sup>York Biomedical Research Institute, University of York, Heslington, York, YO10 5DD, UK

6 \* **Correspondence:** Dr William J. Brackenbury, Department of Biology and York Biomedical  
7 Research Institute, University of York, Wentworth Way, Heslington, York YO10 5DD, UK. Email:  
8 william.brackenbury@york.ac.uk. Tel: +44 1904 328284.

9 Keywords: Anticonvulsant, cancer, epilepsy, eslicarbazepine acetate, Na<sub>v</sub>1.5, S-licarbazepine,  
10 voltage-gated Na<sup>+</sup> channel.

## 11 **Abstract**

12 Eslicarbazepine acetate (ESL) is a dibenzazepine anticonvulsant approved as adjunctive treatment for  
13 partial-onset epileptic seizures. Following first pass hydrolysis of ESL, S-licarbazepine (S-Lic)  
14 represents around 95 % of circulating active metabolites. S-Lic is the main enantiomer responsible  
15 for anticonvulsant activity and this is proposed to be through the blockade of voltage-gated Na<sup>+</sup>  
16 channels (VGSCs). ESL and S-Lic both have a voltage-dependent inhibitory effect on the Na<sup>+</sup> current  
17 in N1E-115 neuroblastoma cells expressing neuronal VGSC subtypes including Na<sub>v</sub>1.1, Na<sub>v</sub>1.2,  
18 Na<sub>v</sub>1.3, Na<sub>v</sub>1.6 and Na<sub>v</sub>1.7. ESL has not been associated with cardiotoxicity in healthy volunteers,  
19 although a prolongation of the electrocardiographic PR interval has been observed, suggesting that  
20 ESL may also inhibit cardiac Na<sub>v</sub>1.5 isoform. However, this has not previously been studied. Here,  
21 we investigated the electrophysiological effects of ESL and S-Lic on Na<sub>v</sub>1.5 using whole-cell patch  
22 clamp recording. We interrogated two model systems: (1) MDA-MB-231 metastatic breast  
23 carcinoma cells, which endogenously express the ‘neonatal’ Na<sub>v</sub>1.5 splice variant, and (2) HEK-293  
24 cells stably over-expressing the ‘adult’ Na<sub>v</sub>1.5 splice variant. We show that both ESL and S-Lic  
25 inhibit transient and persistent Na<sup>+</sup> current, hyperpolarise the voltage-dependence of fast inactivation,  
26 and slow the recovery from channel inactivation. These findings highlight, for the first time, the  
27 potent inhibitory effects of ESL and S-Lic on the Na<sub>v</sub>1.5 isoform, suggesting a possible explanation  
28 for the prolonged PR interval observed in patients on ESL treatment. Given that numerous cancer  
29 cells have also been shown to express Na<sub>v</sub>1.5, and that VGSCs potentiate invasion and metastasis,  
30 this study also paves the way for future investigations into ESL and S-Lic as potential invasion  
31 inhibitors.

## 32 **1 Introduction**

33 Eslicarbazepine acetate (ESL) is a member of the dibenzazepine anticonvulsant family of compounds  
34 which also includes oxcarbazepine and carbamazepine (1). ESL has been approved by the European  
35 Medicines Agency and the United States Federal Drug Administration as an adjunctive treatment for  
36 partial-onset epileptic seizures (2). ESL is administered orally and rapidly undergoes first pass  
37 hydrolysis to two stereoisomeric metabolites, R-licarbazepine and S-licarbazepine (S-Lic; also known  
38 as eslicarbazepine; Figure 1A, B) (3-5). S-Lic represents around 95 % of circulating active  
39 metabolites following first pass hydrolysis of ESL and is the enantiomer responsible for

40 anticonvulsant activity (6, 7). S-Lic also has improved blood brain barrier penetration compared to R-  
41 licarbazepine (8). Although S-Lic has been shown to inhibit T type Ca<sup>2+</sup> channels (9), its main  
42 activity is likely through blockade of voltage-gated Na<sup>+</sup> channels (VGSCs) (10). ESL offers several  
43 clinical advantages over other older VGSC-inhibiting antiepileptic drugs, e.g. carbamazepine,  
44 phenytoin; it has a favourable safety profile (10, 11), reduced induction of hepatic cytochrome P450  
45 enzymes (12), low potential for drug-drug interactions (13, 14), and takes less time to reach a steady  
46 state plasma concentration (15).

47 VGSCs are composed of a pore-forming  $\alpha$  subunit in association with one or more auxiliary  $\beta$   
48 subunits, the latter modulating channel gating and kinetics in addition to functioning as cell adhesion  
49 molecules (16). There are nine  $\alpha$  subunits (Na<sub>v</sub>1.1-Na<sub>v</sub>1.9), and four  $\beta$  subunits ( $\beta$ 1-4) (17, 18). In  
50 postnatal and adult CNS neurons, the predominant  $\alpha$  subunits are the tetrodotoxin-sensitive Na<sub>v</sub>1.1,  
51 Na<sub>v</sub>1.2 and Na<sub>v</sub>1.6 isoforms (19) and it is therefore on these that the VGSC-inhibiting activity of ESL  
52 and S-Lic has been described. In the murine neuroblastoma N1E-115 cell line, which expresses  
53 Na<sub>v</sub>1.1, Na<sub>v</sub>1.2, Na<sub>v</sub>1.3, Na<sub>v</sub>1.6 and Na<sub>v</sub>1.7, ESL and S-Lic both have a voltage-dependent inhibitory  
54 effect on the Na<sup>+</sup> current (10, 20). In this cell model, S-Lic has no effect on the voltage-dependence  
55 of fast inactivation, but significantly hyperpolarises the voltage-dependence of slow inactivation (10).  
56 S-Lic also has a lower affinity for VGSCs in the resting state than carbamazepine or oxcarbazepine,  
57 thus potentially improving its therapeutic window over first- and second-generation dibenzazepine  
58 compounds (10). In acutely isolated murine hippocampal CA1 neurons, which express Na<sub>v</sub>1.1,  
59 Na<sub>v</sub>1.2 and Na<sub>v</sub>1.6 (21-23), S-Lic significantly reduces the persistent Na<sup>+</sup> current, a very slow-  
60 inactivating component ~1 % the size of the peak transient Na<sup>+</sup> current (24, 25). Moreover, in  
61 contrast to carbamazepine, this effect is maintained in the absence of  $\beta$ 1 (24, 26).

62 In healthy volunteers, ESL has not been associated with cardiotoxicity and the QT interval remains  
63 unchanged on treatment (27). However, a prolongation of the PR interval has been observed (27),  
64 suggesting that caution should be exercised in patients with cardiac conduction abnormalities (13).  
65 Prolongation of the PR interval suggests that ESL may also inhibit the cardiac Na<sub>v</sub>1.5 isoform,  
66 although this has not previously been studied. Na<sub>v</sub>1.5 is not only responsible for the initial  
67 depolarisation of the cardiac action potential (28), but is also expressed in breast and colon carcinoma  
68 cells, where the persistent Na<sup>+</sup> current promotes invasion and metastasis (29-32). Inhibition of Na<sub>v</sub>1.5  
69 with phenytoin or ranolazine decreases tumour growth, invasion and metastasis (33-35). Thus, it is of  
70 interest to specifically understand the effect of ESL on the Na<sub>v</sub>1.5 isoform.

71 In the present study we investigated the electrophysiological effects of ESL and S-Lic on Na<sub>v</sub>1.5 [1]  
72 endogenously expressed in the MDA-MB-231 metastatic breast carcinoma cell line, and [2] stably  
73 over-expressed in HEK-293 cells. We show that both ESL and S-Lic inhibit transient and persistent  
74 Na<sup>+</sup> current, hyperpolarise the voltage-dependence of fast inactivation, and slow the recovery from  
75 channel inactivation. These findings highlight, for the first time, the potent inhibitory effects of ESL  
76 and S-Lic on the Na<sub>v</sub>1.5 isoform.

## 77 **2 Materials and methods**

### 78 **2.1 Pharmacology**

79 ESL (Tokyo Chemical Industry UK Ltd) was dissolved in DMSO to make a stock concentration of  
80 67 mM. S-Lic (Tocris) was dissolved in DMSO to make a stock concentration of 300 mM. Both  
81 drugs were diluted to a working concentration of 300  $\mu$ M in extracellular recording solution. The  
82 concentration of DMSO in the recording solution was 0.45 % for ESL and 0.1 % for S-Lic. Equal

83 concentrations of DMSO were used in the control solutions. DMSO (0.45 %) had no effect on the  
84 Na<sup>+</sup> current (Supplementary Figure 1).

## 85 **2.2 Cell culture**

86 MDA-MB-231 cells and HEK-293 cells stably expressing Nav1.5 (a gift from L. Isom, University of  
87 Michigan) were grown in Dulbecco's modified eagle medium supplemented with 5 % FBS and 4  
88 mM L-glutamine (36). Molecular identity of the MDA-MB-231 cells was confirmed by short tandem  
89 repeat analysis (37). Cells were confirmed as mycoplasma-free using the DAPI method (38). Cells  
90 were seeded onto glass coverslips 48 h before electrophysiological recording.

## 91 **2.3 Electrophysiology**

92 Plasma membrane Na<sup>+</sup> currents were recorded using the whole-cell patch clamp technique, using  
93 methods described previously (32, 35). Patch pipettes made of borosilicate glass were pulled using a  
94 P-97 pipette puller (Sutter Instrument) and fire-polished to a resistance of 3-5 MΩ when filled with  
95 intracellular recording solution. The extracellular recording solution for MDA-MB-231 cells  
96 contained (in mM): 144 NaCl, 5.4 KCl, 1 MgCl<sub>2</sub>, 2.5 CaCl<sub>2</sub>, 5.6 D-glucose and 5 HEPES (adjusted to  
97 pH 7.2 with NaOH). For the extracellular recording solution for HEK-293 cells expressing Nav1.5,  
98 the extracellular [Na<sup>+</sup>] was reduced to account for the much larger Na<sup>+</sup> currents and contained (in  
99 mM): 60 NaCl, 84 Choline Cl, 5.4 KCl, 1 MgCl<sub>2</sub>, 2.5 CaCl<sub>2</sub>, 5.6 D-glucose and 5 HEPES (adjusted  
100 to pH 7.2 with NaOH). The intracellular recording solution contained (in mM): 5 NaCl, 145 CsCl, 2  
101 MgCl<sub>2</sub>, 1 CaCl<sub>2</sub>, 10 HEPES, 11 EGTA, (adjusted to pH 7.4 with CsOH) (39). Voltage clamp  
102 recordings were made at room temperature using a Multiclamp 700B amplifier (Molecular Devices)  
103 compensating for series resistance by 40–60%. Currents were digitized using a Digidata 1440A  
104 interface (Molecular Devices), low pass filtered at 10 kHz, sampled at 50 kHz and analysed using  
105 pCLAMP 10.7 software (Molecular Devices). Leak current was subtracted using a P/6 protocol (40).  
106 Extracellular recording solution ± drugs was applied to the recording bath at a rate of ~1.5 ml/min  
107 using a ValveLink 4-channel gravity perfusion controller (AutoMate Scientific). Each new solution  
108 was allowed to equilibrate in the bath for ~4 min following switching prior to recording at steady  
109 state.

## 110 **2.4 Voltage clamp protocols**

111 Cells were clamped at a holding potential of -120 mV or -80 mV for ≥ 250 ms, dependent on  
112 experiment (detailed in the Figure legends). Five main voltage clamp protocols were used, as  
113 follows:

- 114 1. To assess the effect of drug perfusion and wash-out on peak current in real time, a simple one-  
115 step protocol was used where cells were held at -120 mV or -80 mV for 250 ms and then  
116 depolarised to -10 mV for 50 ms.
- 117 2. To assess the voltage-dependence of activation, cells were held at -120 mV for 250 ms and then  
118 depolarised to test potentials in 10 mV steps between -120 mV and +30 mV for 50 ms. The  
119 voltage of activation was taken as the most negative voltage which induced a visible transient  
120 inward current.
- 121 3. To assess the voltage-dependence of steady-state inactivation, cells were held at -120 mV for 250  
122 ms followed by prepulses for 250 ms in 10 mV steps between -120 mV and +30 mV and a test  
123 pulse to -10 mV for 50 ms.

- 124 4. To assess use-dependent block, cells were held at -120 mV for 250 ms and then depolarised to 0  
125 mV at a frequency of 50 Hz, with each depolarisation pulse lasting 5 ms.
- 126 5. To assess recovery from fast inactivation, cells were held at -120 mV for 250 ms, and then  
127 depolarised twice to 0 mV for 25 ms, returning to -120 mV for the following intervals between  
128 depolarisations (in ms): 1, 2, 3, 5, 7, 10, 15, 20, 30, 40, 50, 70, 100, 150, 200, 250, 350, 500. In  
129 each case, the second current was normalised to the initial current and plotted against the interval  
130 time.

## 131 **2.5 Curve fitting and data analysis**

132 To study the voltage-dependence of activation, current-voltage (I-V) relationships were converted to  
133 conductance using the following equation:

134  $G = I / (V_m - V_{rev})$ , where  $G$  is conductance,  $I$  is current,  $V_m$  is the membrane voltage and  $V_{rev}$   
135 is the reversal potential for Na<sup>+</sup> derived from the Nernst equation. Given the different recording  
136 solutions used,  $V_{rev}$  for Na<sup>+</sup> was +85 mV for MDA-MB-231 cells and +63 mV for HEK-Nav1.5 cells.

137 The voltage-dependence of conductance and availability were normalised and fitted to a Boltzmann  
138 equation:

139  $G = G_{max} / (1 + \exp((V_{1/2} - V_m) / k))$ , where  $G_{max}$  is the maximum conductance,  $V_{1/2}$  is the  
140 voltage at which the channels are half activated/inactivated,  $V_m$  is the membrane voltage and  $k$  is the  
141 slope factor.

142 Recovery from inactivation data ( $I_t / I_{t=0}$ ) were normalised, plotted against recovery time ( $\Delta t$ ) and  
143 fitted to a single exponential function:

144  $\tau = A_1 + A_2 \exp(-t / t_0)$ , where  $A_1$  and  $A_2$  are the coefficients of decay of the time constant  
145 ( $\tau$ ),  $t$  is time and  $t_0$  is a time constant describing the time dependence of  $\tau$ .

146 The time course of inactivation was fitted to a double exponential function:

147  $I = A_f \exp(-t / \tau_f) + A_s \exp(-t / \tau_s) + C$ , where  $A_f$  and  $A_s$  are maximal amplitudes of the slow  
148 and fast components of the current,  $\tau_f$  and  $\tau_s$  are the fast and slow decay time constants and  $C$  is the  
149 asymptote.

## 150 **2.6 Statistical analysis**

151 Data are presented as mean and SEM unless stated otherwise. Statistical analysis was performed on  
152 the raw data using GraphPad Prism 8.4.0. Pairwise statistical significance was determined with  
153 Student's paired  $t$ -tests. Multiple comparisons were made using ANOVA and Tukey post-hoc tests,  
154 unless stated otherwise. Results were considered significant at  $P < 0.05$ .

## 155 **3 Results**

### 156 **3.1 Effect of eslicarbazepine acetate and S-licarbazepine on transient and persistent Na<sup>+</sup> 157 current**

158 Several studies have clearly established the inhibition of neuronal VGSCs (Na<sub>v</sub>1.1, Na<sub>v</sub>1.2, Na<sub>v</sub>1.3,  
159 Na<sub>v</sub>1.6, Na<sub>v</sub>1.7 and Na<sub>v</sub>1.8) by ESL and its active metabolite S-Lic (10, 20, 24, 41). Given that ESL

160 prolongs the PR interval (27), potentially via inhibiting the cardiac Na<sub>v</sub>1.5 isoform, together with the  
161 interest in inhibiting Na<sub>v</sub>1.5 in carcinoma cells to reduce invasion and metastasis (33, 34, 42-44), it is  
162 also relevant to evaluate the electrophysiological effects of ESL and S-Lic on this isoform. We  
163 therefore evaluated the effect of both compounds on Na<sub>v</sub>1.5 current properties using whole-cell patch  
164 clamp recording, employing a two-pronged approach: (1) recording Na<sub>v</sub>1.5 currents endogenously  
165 expressed in the MDA-MB-231 breast cancer cell line (29, 30, 45), and (2) recording from Na<sub>v</sub>1.5  
166 stably over-expressed in HEK-293 cells (HEK-Na<sub>v</sub>1.5) (46).

167 Initially, we evaluated the effect of both compounds on the size of the peak Na<sup>+</sup> current in MDA-  
168 MB-231 cells. Na<sup>+</sup> currents were elicited by depolarising the membrane potential ( $V_m$ ) to -10 mV  
169 from a holding potential ( $V_h$ ) of -120 mV or -80 mV. Application of the prodrug ESL (300 μM)  
170 reversibly inhibited the transient Na<sup>+</sup> current by  $49.6 \pm 3.2$  % when the  $V_h$  was -120 mV ( $P < 0.001$ ;  
171  $n = 13$ ; ANOVA + Tukey test; Figure 2A, D). When  $V_h$  was set to -80 mV, ESL reversibly inhibited  
172 the transient Na<sup>+</sup> current by  $79.5 \pm 4.5$  % ( $P < 0.001$ ;  $n = 12$ ; ANOVA + Tukey test; Figure 2C, E).  
173 We next assessed the effect of ESL in HEK-Na<sub>v</sub>1.5 cells. Application of ESL inhibited Na<sub>v</sub>1.5  
174 current by  $74.7 \pm 4.3$  % when  $V_h$  was -120 mV ( $P < 0.001$ ;  $n = 12$ ; Figure 2F, I) and by  $90.5 \pm 2.8$  %  
175 when  $V_h$  was -80 mV ( $P < 0.001$ ;  $n = 14$ ; Figure 2H, J). However, the inhibition was only partially  
176 reversible ( $P < 0.001$ ;  $n = 14$ ; Figure 2F, H-J). Together, these data suggest that ESL preferentially  
177 inhibited Na<sub>v</sub>1.5 in the open or inactivated state, since the current inhibition was greater at more  
178 depolarised  $V_h$ .

179 We next tested the effect of the active metabolite S-Lic. S-Lic (300 μM) inhibited the transient Na<sup>+</sup>  
180 current in MDA-MB-231 cells by  $44.4 \pm 6.1$  % when the  $V_h$  was -120 mV ( $P < 0.001$ ;  $n = 9$ ;  
181 ANOVA + Tukey test; Figure 3A, D). When  $V_h$  was set to -80 mV, S-Lic (300 μM) inhibited the  
182 transient Na<sup>+</sup> current by  $73.6 \pm 4.1$  % ( $P < 0.001$ ;  $n = 10$ ; ANOVA + Tukey test; Figure 3C, E).  
183 However, the inhibition caused by S-Lic was only partially reversible ( $P < 0.05$ ;  $n = 10$ ; ANOVA +  
184 Tukey test; Figure 3A, C-E). In HEK-Na<sub>v</sub>1.5 cells, S-Lic inhibited Na<sub>v</sub>1.5 current by  $46.4 \pm 3.9$  %  
185 when  $V_h$  was -120 mV ( $P < 0.001$ ;  $n = 13$ ; ANOVA + Tukey test; Figure 3F, I) and by  $74.0 \pm 4.2$  %  
186 when  $V_h$  was -80 mV ( $P < 0.001$ ;  $n = 12$ ; ANOVA + Tukey test; Figure 3H, J). Furthermore, the  
187 inhibition in HEK-Na<sub>v</sub>1.5 cells was not reversible over the duration of the experiment. Together,  
188 these data show that channel inhibition by S-Lic was also more effective at more depolarised  $V_h$ .  
189 However, unlike ESL, channel blockade by S-Lic persisted after washout, suggesting higher target  
190 binding affinity for the active metabolite.

191 We also assessed the effect of both compounds on the persistent Na<sup>+</sup> current measured 20-25 ms after  
192 depolarisation to -10 mV from -120 mV. In MDA-MB-231 cells, ESL inhibited the persistent Na<sup>+</sup>  
193 current by  $77 \pm 34$  % although the reduction was not statistically significant ( $P = 0.13$ ;  $n = 12$ ; paired  
194 t test; Figure 2B, Table 1). In HEK-Na<sub>v</sub>1.5 cells, ESL inhibited persistent current by  $76 \pm 10$  % ( $P <$   
195  $0.01$ ;  $n = 12$ ; paired t test; Figure 2G, Table 1). S-Lic inhibited the persistent Na<sup>+</sup> current in MDA-  
196 MB-231 cells by  $66 \pm 16$  % ( $P < 0.05$ ;  $n = 9$ ; paired t test; Figure 3B, Table 2). In HEK-Na<sub>v</sub>1.5 cells,  
197 S-Lic inhibited persistent current by  $35 \pm 16$  % ( $P < 0.05$ ;  $n = 11$ ; Figure 3G, Table 2). In summary,  
198 both ESL and S-Lic also inhibited the persistent Na<sup>+</sup> current.

### 199 **3.2 Effect of eslicarbazepine acetate and S-licarbazepine on voltage dependence of activation** 200 **and inactivation**

201 We next investigated the effect of ESL (300 μM) and S-Lic (300 μM) on the I-V relationship in  
202 MDA-MB-231 and HEK-Na<sub>v</sub>1.5 cells. A  $V_h$  of -120 mV was used for subsequent analyses to ensure  
203 that the elicited currents were sufficiently large for analysis of kinetics and voltage dependence,

204 particularly for MDA-MB-231 cells, which display smaller peak Na<sup>+</sup> currents (Tables 1, 2). Neither  
205 ESL nor S-Lic had any effect on the threshold voltage for activation (Figure 4A-D; Tables 1, 2). ESL  
206 also had no effect on the voltage at current peak in either cell line (Figure 4A-D; Tables 1, 2).  
207 Although S-Lic had no effect on voltage at current peak in MDA-MB-231 cells, it significantly  
208 hyperpolarised in HEK-Na<sub>v</sub>1.5 cells from  $-18.0 \pm 4.2$  mV to  $-30.0 \pm 5.6$  mV ( $P < 0.001$ ;  $n = 9$ ; paired  
209 t test; Figure 4A-D; Tables 1, 2).

210 ESL had no significant effect on the half-activation voltage ( $V_{1/2}$ ) or slope factor ( $k$ ) for activation in  
211 MDA-MB-231 cells (Figure 5A; Table 1). The activation  $k$  in HEK-Na<sub>v</sub>1.5 cells was also unchanged  
212 but the activation  $V_{1/2}$  was significantly hyperpolarised by ESL from  $-39.4 \pm 1.3$  to  $-44.2 \pm 1.8$  mV ( $P$   
213  $< 0.05$ ;  $n = 10$ ; paired t test; Figure 5B; Table 1). S-Lic also had no significant effect on the activation  
214  $V_{1/2}$  or  $k$  in MDA-MB-231 cells (Figure 5C; Table 2). However, the  $V_{1/2}$  of activation in HEK-Na<sub>v</sub>1.5  
215 cells was significantly hyperpolarised from  $-32.8 \pm 3.1$  mV to  $-40.5 \pm 3.4$  mV ( $P < 0.01$ ;  $n = 9$ ; paired  
216 t test; Figure 5D; Table 2) and  $k$  changed from  $5.9 \pm 0.9$  mV to  $4.5 \pm 1.1$  mV ( $P < 0.05$ ;  $n = 9$ ; paired  
217 t test; Figure 5D; Table 2).

218 As regards steady-state inactivation, in MDA-MB-231 cells, ESL significantly hyperpolarised the  
219 inactivation  $V_{1/2}$  from  $-80.6 \pm 0.7$  mV to  $-86.7 \pm 1.2$  mV ( $P < 0.001$ ;  $n = 13$ ; paired t test) without  
220 affecting inactivation  $k$  (Figure 5A; Table 1). ESL also hyperpolarised the inactivation  $V_{1/2}$  in HEK-  
221 Na<sub>v</sub>1.5 cells from  $-78.2 \pm 2.5$  mV to  $-88.3 \pm 2.7$  mV ( $P < 0.001$ ;  $n = 10$ ; paired t test), and changed  
222 the inactivation  $k$  from  $-6.9 \pm 0.4$  mV to  $-9.8 \pm 0.7$  mV ( $P < 0.001$ ;  $n = 10$ ; paired t test; Figure 5B;  
223 Table 1). S-Lic also significantly hyperpolarised the inactivation  $V_{1/2}$  in MDA-MB-231 cells from -  
224  $71.8 \pm 2.5$  mV to  $-76.8 \pm 2.2$  mV ( $P < 0.05$ ;  $n = 7$ ; paired t test) without affecting inactivation  $k$   
225 (Figure 5C; Table 2). However, the inactivation  $V_{1/2}$  in HEK-Na<sub>v</sub>1.5 cells was not significantly  
226 altered by S-Lic, although the inactivation  $k$  significantly changed from  $-6.5 \pm 0.4$  mV to  $-8.1 \pm 0.5$   
227 mV ( $P < 0.05$ ;  $n = 9$ ; paired t test; Figure 5D; Table 2). In summary, both ESL and S-Lic affected  
228 various aspects of the voltage dependence characteristics of Na<sub>v</sub>1.5 in MDA-MB-231 and HEK-  
229 Na<sub>v</sub>1.5 cells, predominantly hyperpolarising the voltage dependence of inactivation.

### 230 **3.3 Effect of eslicarbazepine acetate and S-licarbazepine on activation and inactivation** 231 **kinetics**

232 We next studied the effect of both compounds on kinetics of activation and inactivation. In MDA-  
233 MB-231 cells, ESL significantly accelerated the time to peak current ( $T_p$ ) upon depolarisation from  
234  $-120$  mV to  $-10$  mV from  $2.1 \pm 0.2$  ms to  $1.9 \pm 0.2$  ms ( $P < 0.01$ ;  $n = 13$ ; paired t test; Table 1).  
235 However, in HEK-Na<sub>v</sub>1.5 cells, ESL significantly slowed  $T_p$  from  $1.4 \pm 0.2$  ms to  $1.5 \pm 0.2$  ms ( $P <$   
236  $0.001$ ;  $n = 14$ ; paired t test; Table 1). S-Lic had no significant effect on  $T_p$  in MDA-MB-231 cells but  
237 significantly slowed  $T_p$  in HEK-Na<sub>v</sub>1.5 cells from  $1.8 \pm 0.5$  ms to  $2.3 \pm 0.6$  ms ( $P < 0.01$ ;  $n = 13$ ;  
238 paired t test; Table 2).

239 To study effects on inactivation kinetics, the current decay following depolarisation from  $-120$  mV to  
240  $-10$  mV was fitted to a double exponential function to derive fast and slow time constants of  
241 inactivation ( $\tau_f$  and  $\tau_s$ ). Neither ESL nor S-Lic had any significant effect on  $\tau_f$  or  $\tau_s$  in MDA-MB-231  
242 cells (Tables 1, 2). However, in HEK-Na<sub>v</sub>1.5 cells, ESL significantly slowed  $\tau_f$  from  $0.9 \pm 0.1$  ms to  
243  $1.2 \pm 0.1$  ms ( $P < 0.001$ ;  $n = 12$ ; paired t test; Table 1) and slowed  $\tau_s$  from  $6.6 \pm 0.8$  ms to  $20.8 \pm 8.5$   
244 ms, although this was not statistically significant. S-Lic significantly slowed  $\tau_f$  from  $1.0 \pm 0.04$  ms to  
245  $1.3 \pm 0.06$  ms ( $P < 0.001$ ;  $n = 11$ ; paired t test; Table 2) and  $\tau_s$  from  $6.3 \pm 0.5$  ms to  $7.3 \pm 0.5$  ms ( $P <$   
246  $0.05$ ;  $n = 11$ ; paired t test; Table 2). In summary, both ESL and S-Lic elicited various effects on  
247 kinetics in MDA-MB-231 and HEK-Na<sub>v</sub>1.5 cells, predominantly slowing activation and inactivation.

### 248 3.4 Use-dependent effect of eslicarbazepine acetate and S-licarbazepine on Na<sub>v</sub>1.5

249 To study use-dependent block of Na<sup>+</sup> current by ESL and S-Lic, we ran a protocol where cells were  
250 subjected to repeated depolarisations from -120 mV to 0 mV, at a frequency of 50 Hz. In MDA-MB-  
251 231 cells, this depolarisation train caused a rapid decrease in current size, which reached a plateau of  
252 88.8 ± 2.3 % of the initial current (Figure 6A). In the presence of ESL, the decrease in current  
253 reached a plateau of 81.5 ± 2.3 %, suggesting use-dependent block of the channel, although this was  
254 not statistically significant (P = 0.10; n = 9; paired t test; Figure 6A). S-Lic had a similar but less  
255 obvious effect where the current declined to 80.5 ± 3.1 % in the presence of S-Lic, compared to 86.5  
256 ± 3.1 % without drug (P = 0.31; n = 7; paired t test; Figure 6B).

257 Use-dependent block was easier to study in HEK-Na<sub>v</sub>1.5 cells due to the larger Na<sup>+</sup> current. In these  
258 cells, ESL increased the reduction in current amplitude to 60.6 ± 7.9 % of the initial current,  
259 compared to 90.0 ± 2.1 % without drug (P < 0.01; n = 9; paired t test; Figure 6C). S-Lic also  
260 increased the reduction in current amplitude to 76.1 ± 2.1 % of the initial current, compared to 85.7 ±  
261 2.2 % without drug (P < 0.001; n = 9; paired t test; Figure 6D). Together, these results indicate that  
262 both ESL and S-Lic cause use-dependent block of Na<sub>v</sub>1.5 at a stimulation frequency of 50 Hz.

### 263 3.5 Effect of eslicarbazepine acetate and S-licarbazepine on recovery from fast inactivation

264 To investigate the effect of ESL and S-Lic on channel recovery from fast inactivation, we subjected  
265 cells to two depolarisations from V<sub>h</sub> of -120 mV to 0 mV, changing the interval between these in  
266 which the channels were held at -120 mV to facilitate recovery. Significance was determined by  
267 fitting a single exponential curve to the normalised current/time relationship and calculating the time  
268 constant (τ<sub>r</sub>). In MDA-MB-231 cells, ESL significantly slowed τ<sub>r</sub> from 6.0 ± 0.5 ms to 8.7 ± 0.7 ms  
269 (P < 0.05; n = 10; paired t test; Figure 7A, Table 1). Similarly, in HEK-Na<sub>v</sub>1.5 cells, ESL  
270 significantly slowed τ<sub>r</sub> from 4.5 ± 0.4 ms to 7.1 ± 0.6 ms (P < 0.001; n = 10; paired t test; Figure 7B,  
271 Table 1). S-Lic also significantly slowed τ<sub>r</sub> in MDA-MB-231 cells from 6.8 ± 0.4 ms to 13.5 ± 1.0  
272 ms (P < 0.01; n = 7; paired t test; Figure 7C, Table 2). Finally, S-Lic also significantly slowed τ<sub>r</sub> in  
273 HEK-Na<sub>v</sub>1.5 cells from 5.7 ± 0.7 ms to 8.0 ± 1.2 ms (P < 0.01; n = 10; paired t test; Figure 7D, Table  
274 2). In summary, both ESL and S-Lic slowed recovery from fast inactivation of Na<sub>v</sub>1.5.

## 275 4 Discussion

276 In this study, we have shown that ESL and its active metabolite S-Lic (both at 300 μM) inhibit the  
277 transient and persistent components of Na<sup>+</sup> current carried by Na<sub>v</sub>1.5. We show broadly similar  
278 effects in MDA-MB-231 cells, which express endogenous Na<sub>v</sub>1.5 (29, 30, 45), and in HEK-293 cells  
279 over-expressing Na<sub>v</sub>1.5. Notably, both compounds were more effective when V<sub>h</sub> was set to -80 mV  
280 than at -120 mV, suggestive of depolarised state-dependent binding. In addition, the inhibitory effect  
281 of ESL was reversible whereas inhibition by S-Lic was not. As regards voltage-dependence, both  
282 ESL and S-Lic shifted activation and steady-state inactivation curves, to varying extents in the two  
283 cell lines, in the direction of more negative voltages. ESL and S-Lic had various effects on activation  
284 and inactivation kinetics, generally slowing the rate of inactivation. Both ESL and S-Lic also caused  
285 use-dependent block of Na<sub>v</sub>1.5, although the effect was more obvious in HEK-Na<sub>v</sub>1.5 cells due to the  
286 larger Na<sup>+</sup> current. Finally, recovery from fast inactivation of Na<sub>v</sub>1.5 was significantly slowed by  
287 both ESL and S-Lic.

288 To our knowledge, this is the first time that the effects of ESL and S-Lic have specifically been tested  
289 on the Na<sub>v</sub>1.5 isoform. A strength of this study is that both the prodrug (ESL) and the active  
290 metabolite (S-Lic) were tested using two independent cell lines, one endogenously expressing

291 Na<sub>v</sub>1.5, the other stably over-expressing Na<sub>v</sub>1.5. MDA-MB-231 cells also express Na<sub>v</sub>1.7, although  
292 this isoform is estimated to be responsible for only ~9 % of the total VGSC current (30, 45). MDA-  
293 MB-231 cells also express endogenous β<sub>1</sub>, β<sub>2</sub> and β<sub>4</sub> subunits (47-49). MDA-MB-231 cells  
294 predominantly express the developmentally regulated ‘neonatal’ Na<sub>v</sub>1.5 splice variant, which differs  
295 from the ‘adult’ variant over-expressed in the HEK-Na<sub>v</sub>1.5 cells by seven amino acids located in the  
296 extracellular linker between transmembrane segments 3 and 4 of domain 1 (30, 42, 45). Notably,  
297 however, there were no consistent differences in effect of either ESL or S-Lic between the MDA-  
298 MB-231 and HEK-Na<sub>v</sub>1.5 cells, suggesting that the neonatal vs. adult splicing event, and/or  
299 expression of endogenous β subunits, does not impact on sensitivity of Na<sub>v</sub>1.5 to these compounds.  
300 This finding contrasts another report showing different sensitivity of the neonatal and adult Na<sub>v</sub>1.5  
301 splice variants to the amide local anaesthetics lidocaine and levobupivacaine (44). Our findings  
302 suggest that the inhibitory effect of S-Lic on Na<sub>v</sub>1.5 is less reversible than that of ESL. This may be  
303 explained by the differing chemical structures of the two molecules possibly enabling S-Lic to bind  
304 the target with higher affinity than ESL. Most VGSC-targeting anticonvulsants, including phenytoin,  
305 lamotrigine and carbamazepine, block the pore by binding via aromatic-aromatic interaction to a  
306 tyrosine and phenylalanine located in the S6 helix of domain 4 (50). However, S-Lic has been  
307 proposed to bind to a different site given that it was found to block the pore predominantly during  
308 slow inactivation (10). Alternatively, the hydroxyl group present on S-Lic (but not ESL) may become  
309 deprotonated, potentially trapping it in the cytoplasm.

310 This study used a single concentration for both compounds (300 μM) and the findings presented here  
311 broadly agree with *in vitro* concentrations used elsewhere to study effects of ESL and S-Lic on Na<sup>+</sup>  
312 currents. For example, using a V<sub>h</sub> of -80 mV, 300 μM ESL was shown to inhibit peak Na<sup>+</sup> current by  
313 50 % in N1E-115 neuroblastoma cells expressing Na<sub>v</sub>1.1, Na<sub>v</sub>1.2, Na<sub>v</sub>1.3, Na<sub>v</sub>1.6 and Na<sub>v</sub>1.7 (20). S-  
314 Lic (250 μM) also blocks peak Na<sup>+</sup> current by ~50 % in the same cell line (10). In addition, S-Lic  
315 (300 μM) reduces persistent Na<sup>+</sup> current by ~25 % in acutely isolated murine hippocampal CA1  
316 neurons expressing Na<sub>v</sub>1.1, Na<sub>v</sub>1.2 and Na<sub>v</sub>1.6 (21-24). Similar to the present study, ESL was shown  
317 to hyperpolarise the voltage-dependence of steady-state inactivation in N1E-115 cells (20). On the  
318 other hand, similar to our finding in HEK-Na<sub>v</sub>1.5 cells, S-Lic has no effect on steady-state  
319 inactivation in N1E-115 cells (10). Again, in agreement with our own findings for Na<sub>v</sub>1.5, S-Lic  
320 slows recovery from inactivation and causes use-dependent inhibition in N1E-115 cells (10). It  
321 should be noted that the frequency of stimulation used in the protocol to assess use-dependent block  
322 (50 Hz) is much faster than the typical human heart rate (1-2 Hz), thus, Na<sub>v</sub>1.5 in cardiac tissue  
323 would not be expected to experience use-dependent block to this extent. Nonetheless, these  
324 observations suggest that the sensitivity of Na<sub>v</sub>1.5 to ESL and S-Lic is broadly similar to that  
325 reported for neuronal VGSCs. In support of this, Na<sub>v</sub>1.5 shares the same conserved residues proposed  
326 for Na<sub>v</sub>1.2 to interact with ESL (Figure 8) (51).

327 Notably, the concentration used in this study is high compared with concentrations achieved in  
328 clinical use (e.g. ESL 1200 mg QD gives a peak plasma concentration of ~90 μM) (10). However, it  
329 has been argued that the relatively high concentrations required for channel inhibition *in vitro* are  
330 clinically relevant given that S-Lic has a high (50:1) lipid:water partition co-efficient and thus would  
331 be expected to reside predominantly in the tissue membrane fraction *in vivo* (15). Future work  
332 investigating the dose-dependent effects of ESL and S-Lic would be useful to resolve these  
333 possibilities and aid clinical judgements.

334 The data presented here raise several implications for clinicians. The observed tonic and use-  
335 dependent inhibition of Na<sub>v</sub>1.5 is worthy of note when considering cardiac function in patients  
336 receiving ESL (13). Although the QT interval remains unchanged for individuals on ESL treatment,



337 prolongation of the PR interval has been observed (27). Further work is required to establish whether  
338 the basis for this PR prolongation is indeed via Na<sub>v</sub>1.5 inhibition. In addition, it would be of interest  
339 to investigate the efficacy of ESL and S-Lic in the context of heritable arrhythmogenic mutations in  
340 *SCN5A*, as well as the possible involvement of the  $\beta$  subunits (24, 26, 52, 53). The findings presented  
341 here are also relevant in the context of Na<sub>v</sub>1.5 expression in carcinoma cells (54). Given that cancer  
342 cells have a relatively depolarised  $V_m$ , it is likely that Na<sub>v</sub>1.5 is mainly in the inactivated state with  
343 the persistent Na<sup>+</sup> current being functionally predominant (55, 56). Increasing evidence suggests that  
344 persistent Na<sup>+</sup> current carried by Na<sub>v</sub>1.5 in cancer cells contributes to invasion and several studies  
345 have shown that other VGSC inhibitors reduce metastasis in preclinical models (29-35, 57). Thus,  
346 use-dependent inhibition by ESL would ensure that channels in malignant cells are particularly  
347 targeted, raising the possibility that it could be used as an anti-metastatic agent (43). This study  
348 therefore paves the way for future investigations into ESL and S-Lic as potential invasion inhibitors.

## 349 **5 Author Contributions**

350 TL, SC and WB contributed to the conception and design of the work. TL, LB and WB contributed  
351 to acquisition, analysis, and interpretation of data for the work. TL, SC and WB contributed to  
352 drafting the work and revising it critically for important intellectual content. All authors approved the  
353 final version of the manuscript.

## 354 **6 Abbreviations**

355 ESL, eslicarbazepine acetate; HEK-Na<sub>v</sub>1.5, HEK-293 cells stably expressing Na<sub>v</sub>1.5; I-V, current-  
356 voltage; k, slope factor; PSS, physiological saline solution; S-Lic, S-licarbazepine,  $T_p$ : time to peak  
357 current;  $\tau_f$ : fast time constant of inactivation;  $\tau_s$ : slow time constant of inactivation;  $\tau_r$ : time constant  
358 of recovery from inactivation; VGSC, voltage-gated Na<sup>+</sup> channel;  $V_m$ , membrane potential;  $V_h$ ,  
359 holding potential;  $V_{peak}$ : voltage at which current was maximal;  $V_{rev}$ , reversal potential;  $V_{thres}$ :  
360 threshold voltage for activation;  $V_{1/2}$ , half-activation voltage.

## 361 **7 Acknowledgements**

362 This work was supported by Cancer Research UK (A25922) and Breast Cancer Now  
363 (2015NovPhD572).

## 364 **8 Conflict of interest statement**

365 The authors declare that the research was conducted in the absence of any commercial or financial  
366 relationships that could be construed as a potential conflict of interest.

## 367 **9 Data availability statement**

368 The datasets used and/or analysed during the current study are available from the corresponding  
369 author on reasonable request.

## 370 **10 References**

- 371 1. Almeida L, Soares-da-Silva P. Eslicarbazepine acetate (BIA 2-093). *Neurotherapeutics*.  
372 2007;4(1):88-96.
- 373 2. Sperling MR, Abou-Khalil B, Harvey J, Rogin JB, Biraben A, Galimberti CA, et al.  
374 Eslicarbazepine acetate as adjunctive therapy in patients with uncontrolled partial-onset seizures:

- 375 Results of a phase III, double-blind, randomized, placebo-controlled trial. *Epilepsia*. 2015;56(2):244-  
376 53.
- 377 3. Almeida L, Falcao A, Maia J, Mazur D, Gellert M, Soares-da-Silva P. Single-dose and  
378 steady-state pharmacokinetics of eslicarbazepine acetate (BIA 2-093) in healthy elderly and young  
379 subjects. *J Clin Pharmacol*. 2005;45(9):1062-6.
- 380 4. Almeida L, Minciu I, Nunes T, Butoianu N, Falcão A, Magureanu S-A, et al.  
381 Pharmacokinetics, Efficacy, and Tolerability of Eslicarbazepine Acetate in Children and Adolescents  
382 With Epilepsy. *The Journal of Clinical Pharmacology*. 2008;48(8):966-77.
- 383 5. Perucca E, Elger C, Halász P, Falcão A, Almeida L, Soares-da-Silva P. Pharmacokinetics of  
384 eslicarbazepine acetate at steady-state in adults with partial-onset seizures. *Epilepsy Res*.  
385 2011;96(1):132-9.
- 386 6. Potschka H, Soerensen J, Pekcec A, Loureiro A, Soares-da-Silva P. Effect of eslicarbazepine  
387 acetate in the corneal kindling progression and the amygdala kindling model of temporal lobe  
388 epilepsy. *Epilepsy Res*. 2014;108(2):212-22.
- 389 7. Sierra-Paredes G, Loureiro AI, Wright LC, Sierra-Marcuño G, Soares-da-Silva P. Effects of  
390 eslicarbazepine acetate on acute and chronic latrunculin A-induced seizures and extracellular amino  
391 acid levels in the mouse hippocampus. *BMC Neurosci*. 2014;15(1):134.
- 392 8. Alves G, Figueiredo I, Falcao A, Castel-Branco M, Caramona M, Soares-Da-Silva P.  
393 Stereoselective disposition of S- and R-licarbazepine in mice. *Chirality*. 2008;20(6):796-804.
- 394 9. Brady K, Hebeisen S, Konrad D, Soares-da-Silva P. The effects of eslicarbazepine, R-  
395 licarbazepine, oxcarbazepine and carbamazepine on ion transmission Cav3.2 channels. *Epilepsia*.  
396 2011;52:260.
- 397 10. Hebeisen S, Pires N, Loureiro AI, Bonifacio MJ, Palma N, Whyment A, et al. Eslicarbazepine  
398 and the enhancement of slow inactivation of voltage-gated sodium channels: a comparison with  
399 carbamazepine, oxcarbazepine and lacosamide. *Neuropharmacology*. 2015;89:122-35.
- 400 11. Brown ME, El-Mallakh RS. Role of eslicarbazepine in the treatment of epilepsy in adult  
401 patients with partial-onset seizures. *Ther Clin Risk Manag*. 2010;6:103-9.
- 402 12. Galiana GL, Gauthier AC, Mattson RH. Eslicarbazepine Acetate: A New Improvement on a  
403 Classic Drug Family for the Treatment of Partial-Onset Seizures. *Drugs R D*. 2017;17(3):329-39.
- 404 13. Zaccara G, Giovannelli F, Cincotta M, Carelli A, Verrotti A. Clinical utility of  
405 eslicarbazepine: current evidence. *Drug Des Devel Ther*. 2015;9:781-9.
- 406 14. Falcao A, Fuseau E, Nunes T, Almeida L, Soares-da-Silva P. Pharmacokinetics, drug  
407 interactions and exposure-response relationship of eslicarbazepine acetate in adult patients with  
408 partial-onset seizures: population pharmacokinetic and pharmacokinetic/pharmacodynamic analyses.  
409 *CNS Drugs*. 2012;26(1):79-91.
- 410 15. Bialer M, Soares-da-Silva P. Pharmacokinetics and drug interactions of eslicarbazepine  
411 acetate. *Epilepsia*. 2012;53(6):935-46.
- 412 16. Catterall WA. Structure and function of voltage-gated sodium channels at atomic resolution.  
413 *Exp Physiol*. 2014;99(1):35-51.
- 414 17. Goldin AL, Barchi RL, Caldwell JH, Hofmann F, Howe JR, Hunter JC, et al. Nomenclature  
415 of voltage-gated sodium channels. *Neuron*. 2000;28:365-8.

- 416 18. Brackenbury WJ, Isom LL. Na Channel beta Subunits: Overachievers of the Ion Channel  
417 Family. *Front Pharmacol.* 2011;2:53.
- 418 19. Van Wart A, Matthews G. Impaired firing and cell-specific compensation in neurons lacking  
419 nav1.6 sodium channels. *J Neurosci.* 2006;26(27):7172-80.
- 420 20. Bonifacio MJ, Sheridan RD, Parada A, Cunha RA, Patmore L, Soares-da-Silva P. Interaction  
421 of the novel anticonvulsant, BIA 2-093, with voltage-gated sodium channels: comparison with  
422 carbamazepine. *Epilepsia.* 2001;42(5):600-8.
- 423 21. Royeck M, Horstmann MT, Remy S, Reitze M, Yaari Y, Beck H. Role of axonal Nav1.6  
424 sodium channels in action potential initiation of CA1 pyramidal neurons. *J Neurophysiol.*  
425 2008;100(4):2361-80.
- 426 22. Yu FH, Mantegazza M, Westenbroek RE, Robbins CA, Kalume F, Burton KA, et al. Reduced  
427 sodium current in GABAergic interneurons in a mouse model of severe myoclonic epilepsy in  
428 infancy. *Nat Neurosci.* 2006;9(9):1142-9.
- 429 23. Westenbroek RE, Merrick DK, Catterall WA. Differential subcellular localization of the RI  
430 and RII Na<sup>+</sup> channel subtypes in central neurons. *Neuron.* 1989;3(6):695-704.
- 431 24. Doeser A, Soares-da-Silva P, Beck H, Uebachs M. The effects of eslicarbazepine on  
432 persistent Na(+) current and the role of the Na(+) channel beta subunits. *Epilepsy Res.*  
433 2014;108(2):202-11.
- 434 25. Saint DA. The cardiac persistent sodium current: an appealing therapeutic target? *Br J*  
435 *Pharmacol.* 2008;153(6):1133-42.
- 436 26. Uebachs M, Opitz T, Royeck M, Dickhof G, Horstmann MT, Isom LL, et al. Efficacy loss of  
437 the anticonvulsant carbamazepine in mice lacking sodium channel beta subunits via paradoxical  
438 effects on persistent sodium currents. *J Neurosci.* 2010;30(25):8489-501.
- 439 27. Vaz-Da-Silva M, Nunes T, Almeida L, Gutierrez MJ, Litwin JS, Soares-Da-Silva P.  
440 Evaluation of Eslicarbazepine acetate on cardiac repolarization in a thorough QT/QTc study. *J Clin*  
441 *Pharmacol.* 2012;52(2):222-33.
- 442 28. George AL, Jr. Inherited disorders of voltage-gated sodium channels. *J Clin Invest.*  
443 2005;115(8):1990-9.
- 444 29. Roger S, Besson P, Le Guennec JY. Involvement of a novel fast inward sodium current in the  
445 invasion capacity of a breast cancer cell line. *Biochim Biophys Acta.* 2003;1616(2):107-11.
- 446 30. Fraser SP, Diss JK, Chioni AM, Mycielska ME, Pan H, Yamaci RF, et al. Voltage-gated  
447 sodium channel expression and potentiation of human breast cancer metastasis. *Clin Cancer Res.*  
448 2005;11(15):5381-9.
- 449 31. House CD, Vaske CJ, Schwartz AM, Obias V, Frank B, Luu T, et al. Voltage-gated Na<sup>+</sup>  
450 channel SCN5A is a key regulator of a gene transcriptional network that controls colon cancer  
451 invasion. *Cancer Res.* 2010;70(17):6957-67.
- 452 32. Nelson M, Yang M, Millican-Slater R, Brackenbury WJ. Nav1.5 regulates breast tumor  
453 growth and metastatic dissemination in vivo. *Oncotarget.* 2015;6(32):32914-29.
- 454 33. Nelson M, Yang M, Dowle AA, Thomas JR, Brackenbury WJ. The sodium channel-blocking  
455 antiepileptic drug phenytoin inhibits breast tumour growth and metastasis. *Mol Cancer.*  
456 2015;14(1):13.

- 457 34. Driffort V, Gillet L, Bon E, Marionneau-Lambot S, Oullier T, Joulin V, et al. Ranolazine  
458 inhibits Nav1.5-mediated breast cancer cell invasiveness and lung colonization. *Mol Cancer*.  
459 2014;13(1):264.
- 460 35. Yang M, Kozminski DJ, Wold LA, Modak R, Calhoun JD, Isom LL, et al. Therapeutic  
461 potential for phenytoin: targeting Na(v)1.5 sodium channels to reduce migration and invasion in  
462 metastatic breast cancer. *Breast Cancer Res Treat*. 2012;134(2):603-15.
- 463 36. Simon A, Yang M, Marrison JL, James AD, Hunt MJ, O'Toole PJ, et al. Metastatic breast  
464 cancer cells induce altered microglial morphology and electrical excitability in vivo. *J*  
465 *Neuroinflammation*. 2020;17(1):87.
- 466 37. Masters JR, Thomson JA, Daly-Burns B, Reid YA, Dirks WG, Packer P, et al. Short tandem  
467 repeat profiling provides an international reference standard for human cell lines. *Proc Natl Acad Sci*  
468 *U S A*. 2001;98(14):8012-7.
- 469 38. Uphoff CC, Gignac SM, Drexler HG. Mycoplasma contamination in human leukemia cell  
470 lines. I. Comparison of various detection methods. *J Immunol Methods*. 1992;149(1):43-53.
- 471 39. Brackenbury WJ, Djamgoz MB. Activity-dependent regulation of voltage-gated Na<sup>+</sup> channel  
472 expression in Mat-LyLu rat prostate cancer cell line. *J Physiol*. 2006;573(Pt 2):343-56.
- 473 40. Armstrong CM, Bezanilla F. Inactivation of the sodium channel. II. Gating current  
474 experiments. *J Gen Physiol*. 1977;70(5):567-90.
- 475 41. Soares-da-Silva P, Pires N, Bonifácio MJ, Loureiro AI, Palma N, Wright LC. Eslicarbazepine  
476 acetate for the treatment of focal epilepsy: an update on its proposed mechanisms of action.  
477 *Pharmacol Res Perspect*. 2015;3(2).
- 478 42. Djamgoz MBA, Fraser SP, Brackenbury WJ. In Vivo Evidence for Voltage-Gated Sodium  
479 Channel Expression in Carcinomas and Potentiation of Metastasis. *Cancers (Basel)*. 2019;11(11).
- 480 43. Martin F, Ufodiama C, Watt I, Bland M, Brackenbury WJ. Therapeutic value of voltage-gated  
481 sodium channel inhibitors in breast, colorectal and prostate cancer: a systematic review. *Front*  
482 *Pharmacol*. 2015;6:273.
- 483 44. Elajnaf T, Baptista-Hon DT, Hales TG. Potent Inactivation-Dependent Inhibition of Adult  
484 and Neonatal Nav1.5 Channels by Lidocaine and Levobupivacaine. *Anesth Analg*. 2018;127(3):650-  
485 60.
- 486 45. Brackenbury WJ, Chioni AM, Diss JK, Djamgoz MB. The neonatal splice variant of Nav1.5  
487 potentiates in vitro metastatic behaviour of MDA-MB-231 human breast cancer cells. *Breast Cancer*  
488 *Res Treat*. 2007;101(2):149-60.
- 489 46. Patino GA, Brackenbury WJ, Bao YY, Lopez-Santiago LF, O'Malley HA, Chen CL, et al.  
490 Voltage-Gated Na<sup>+</sup> Channel beta 1B: A Secreted Cell Adhesion Molecule Involved in Human  
491 Epilepsy. *J Neurosci*. 2011;31(41):14577-91.
- 492 47. Nelson M, Millican-Slater R, Forrest LC, Brackenbury WJ. The sodium channel beta1  
493 subunit mediates outgrowth of neurite-like processes on breast cancer cells and promotes tumour  
494 growth and metastasis. *Int J Cancer*. 2014;135(10):2338-51.
- 495 48. Chioni AM, Brackenbury WJ, Calhoun JD, Isom LL, Djamgoz MB. A novel adhesion  
496 molecule in human breast cancer cells: voltage-gated Na<sup>+</sup> channel beta1 subunit. *Int J Biochem Cell*  
497 *Biol*. 2009;41(5):1216-27.

- 498 49. Bon E, Driffort V, Gradek F, Martinez-Caceres C, Anachelin M, Pelegrin P, et al. SCN4B acts  
499 as a metastasis-suppressor gene preventing hyperactivation of cell migration in breast cancer. *Nature*  
500 *communications*. 2016;7:13648.
- 501 50. Lipkind GM, Fozzard HA. Molecular model of anticonvulsant drug binding to the voltage-  
502 gated sodium channel inner pore. *Mol Pharmacol*. 2010;78(4):631-8.
- 503 51. Shaikh S, Rizvi SM, Hameed N, Biswas D, Khan M, Shakil S, et al. Aptiom (eslicarbazepine  
504 acetate) as a dual inhibitor of beta-secretase and voltage-gated sodium channel: advancement in  
505 Alzheimer's disease-epilepsy linkage via an enzoinformatics study. *CNS Neurol Disord Drug*  
506 *Targets*. 2014;13(7):1258-62.
- 507 52. Brackenbury WJ, Isom LL. Voltage-gated Na<sup>+</sup> channels: potential for beta subunits as  
508 therapeutic targets. *Expert Opin Ther Targets*. 2008;12(9):1191-203.
- 509 53. Rivaud MR, Delmar M, Remme CA. Heritable arrhythmia syndromes associated with  
510 abnormal cardiac sodium channel function: ionic and non-ionic mechanisms. *Cardiovasc Res*. 2020.
- 511 54. Fraser SP, Ozerlat-Gunduz I, Brackenbury WJ, Fitzgerald EM, Campbell TM, Coombes RC,  
512 et al. Regulation of voltage-gated sodium channel expression in cancer: hormones, growth factors  
513 and auto-regulation. *Philos Trans R Soc Lond B Biol Sci*. 2014;369(1638):20130105.
- 514 55. Yang M, Brackenbury WJ. Membrane potential and cancer progression. *Front Physiol*.  
515 2013;4:185.
- 516 56. Yang M, James AD, Suman R, Kasprowicz R, Nelson M, O'Toole PJ, et al. Voltage-  
517 dependent activation of Rac1 by Nav 1.5 channels promotes cell migration. *J Cell Physiol*.  
518 2020;235(4):3950-72.
- 519 57. Besson P, Driffort V, Bon E, Gradek F, Chevalier S, Roger S. How do voltage-gated sodium  
520 channels enhance migration and invasiveness in cancer cells? *Biochim Biophys Acta*. 2015;1848(10  
521 Pt B):2493-501.

522

## 523 10.1 Figure legends

524 **Figure 1.** Chemical structures of eslicarbazepine acetate and S-licarbazepine. (A) eslicarbazepine  
525 acetate; (9S)-2-carbamoyl-2-azatricyclo[9.4.0.0<sup>3,8</sup>]pentadeca-1(15),3,5,7,11,13-hexaen-9-yl acetate.  
526 (B) S-licarbazepine; (10R)-10-hydroxy-2-azatricyclo[9.4.0.0<sup>3,8</sup>]pentadeca-1(11),3,5,7,12,14-hexaene-  
527 2-carboxamide. Structures were drawn using Chemspider software.

528 **Figure 2.** Effect of eslicarbazepine acetate on Nav1.5 currents. (A) Representative Na<sup>+</sup> currents in an  
529 MDA-MB-231 cell elicited by a depolarisation from -120 mV to -10 mV in physiological saline  
530 solution (PSS; black), eslicarbazepine acetate (ESL; 300 μM; red) and after washout (grey). Dotted  
531 vertical lines define the persistent Na<sup>+</sup> currents shown in (B). (B) Representative persistent Na<sup>+</sup>  
532 currents in an MDA-MB-231 cell elicited by a depolarisation from -120 mV to -10 mV. (C)  
533 Representative Na<sup>+</sup> currents in an MDA-MB-231 cell elicited by a depolarisation from -80 mV to -10  
534 mV. (D) Normalised Na<sup>+</sup> currents in MDA-MB-231 cells elicited by a depolarisation from -120 mV  
535 to -10 mV. (E) Normalised Na<sup>+</sup> currents in MDA-MB-231 cells elicited by a depolarisation from -80  
536 mV to -10 mV. (F) Representative Na<sup>+</sup> currents in a HEK-Nav1.5 cell elicited by a depolarisation  
537 from -120 mV to -10 mV in PSS (black), ESL (300 μM; red) and after washout (grey). Dotted  
538 vertical lines define the persistent Na<sup>+</sup> currents shown in (G). (G) Representative persistent Na<sup>+</sup>  
539 currents in a HEK-Nav1.5 cell elicited by a depolarisation from -120 mV to -10 mV. (H)

540 Representative Na<sup>+</sup> currents in a HEK-Nav<sub>v</sub>1.5 cell elicited by a depolarisation from -80 mV to -10  
541 mV. (I) Normalised Na<sup>+</sup> currents in HEK-Nav<sub>v</sub>1.5 cells elicited by a depolarisation from -120 mV to -  
542 10 mV. (J) Normalised Na<sup>+</sup> currents in HEK-Nav<sub>v</sub>1.5 cells elicited by a depolarisation from -80 mV to  
543 -10 mV. Results are mean + SEM. \*\*P ≤ 0.01; \*\*\*P ≤ 0.001; one-way ANOVA with Tukey tests (n  
544 = 12-14). NS, not significant.

545 **Figure 3.** Effect of S-licarbazepine on Nav<sub>v</sub>1.5 currents. (A) Representative Na<sup>+</sup> currents in an MDA-  
546 MB-231 cell elicited by a depolarisation from -120 mV to -10 mV in physiological saline solution  
547 (PSS; black), S-licarbazepine (S-Lic; 300 μM; red) and after washout (grey). Dotted vertical lines  
548 define the persistent Na<sup>+</sup> currents shown in (B). (B) Representative persistent Na<sup>+</sup> currents in an  
549 MDA-MB-231 cell elicited by a depolarisation from -120 mV to -10 mV. (C) Representative Na<sup>+</sup>  
550 currents in an MDA-MB-231 cell elicited by a depolarisation from -80 mV to -10 mV. (D)  
551 Normalised Na<sup>+</sup> currents in MDA-MB-231 cells elicited by a depolarisation from -120 mV to -10  
552 mV. (E) Normalised Na<sup>+</sup> currents in MDA-MB-231 cells elicited by a depolarisation from -80 mV to  
553 -10 mV. (F) Representative Na<sup>+</sup> currents in a HEK-Nav<sub>v</sub>1.5 cell elicited by a depolarisation from -120  
554 mV to -10 mV in PSS (black), S-Lic (300 μM; red) and after washout (grey). Dotted vertical lines  
555 define the persistent Na<sup>+</sup> currents shown in (G). (G) Representative persistent Na<sup>+</sup> currents in a HEK-  
556 Nav<sub>v</sub>1.5 cell elicited by a depolarisation from -120 mV to -10 mV. (H) Representative Na<sup>+</sup> currents in  
557 a HEK-Nav<sub>v</sub>1.5 cell elicited by a depolarisation from -80 mV to -10 mV. (I) Normalised Na<sup>+</sup> currents  
558 in HEK-Nav<sub>v</sub>1.5 cells elicited by a depolarisation from -120 mV to -10 mV. (J) Normalised Na<sup>+</sup>  
559 currents in HEK-Nav<sub>v</sub>1.5 cells elicited by a depolarisation from -80 mV to -10 mV. Results are mean  
560 + SEM. \*P ≤ 0.05; \*\*\*P ≤ 0.001; one-way ANOVA with Tukey tests (n = 9-13). NS, not significant.

561 **Figure 4.** Effect of eslicarbazepine acetate and S-licarbazepine on the current-voltage relationship.  
562 (A) Current-voltage (I-V) plots of Na<sup>+</sup> currents in MDA-MB-231 cells in physiological saline  
563 solution (PSS; black circles) and in eslicarbazepine acetate (ESL; 300 μM; red squares). (B) (I-V)  
564 plots of Na<sup>+</sup> currents in HEK-Nav<sub>v</sub>1.5 cells in PSS (black circles) and ESL (300 μM; red squares). (C)  
565 I-V plots of Na<sup>+</sup> currents in MDA-MB-231 cells in PSS (black circles) and S-licarbazepine (S-Lic;  
566 300 μM; red squares). (D) I-V plots of Na<sup>+</sup> currents in HEK-Nav<sub>v</sub>1.5 cells in PSS (black circles) and  
567 S-Lic (300 μM; red squares). Currents were elicited using 10 mV depolarising steps from -80 to +30  
568 mV for 30 ms, from a holding potential of -120 mV. Results are mean ± SEM (n = 7-13).

569 **Figure 5.** Effect of eslicarbazepine acetate and S-licarbazepine on activation and steady-state  
570 inactivation. (A) Activation and steady-state inactivation in MDA-MB-231 cells in physiological  
571 saline solution (PSS; black circles) and in eslicarbazepine acetate (ESL; 300 μM; red squares). (B)  
572 Activation and steady-state inactivation in HEK-Nav<sub>v</sub>1.5 cells in PSS (black circles) and ESL (300  
573 μM; red squares). (C) Activation and steady-state inactivation in MDA-MB-231 cells in PSS (black  
574 circles) and S-licarbazepine (S-Lic; 300 μM; red squares). (D) Activation and steady-state  
575 inactivation in HEK-Nav<sub>v</sub>1.5 cells in PSS (black circles) and S-Lic (300 μM; red squares). For  
576 activation, normalised conductance (G/G<sub>max</sub>) was calculated from the current data and plotted as a  
577 function of voltage. For steady-state inactivation, normalised current (I/I<sub>max</sub>), elicited by 50 ms test  
578 pulses at -10 mV following 250 ms conditioning voltage pulses between -120 mV and +30 mV,  
579 applied from a holding potential of -120 mV, was plotted as a function of the prepulse voltage.  
580 Results are mean ± SEM (n = 7-13). Activation and inactivation curves are fitted with Boltzmann  
581 functions.

582 **Figure 6.** Use-dependent block by eslicarbazepine acetate and S-licarbazepine. (A) Rundown of Na<sup>+</sup>  
583 current in MDA-MB-231 cells in physiological saline solution (PSS; black circles) and in  
584 eslicarbazepine acetate (ESL; 300 μM; red squares). (B) Rundown of Na<sup>+</sup> current in MDA-MB-231

585 cells in PSS (black circles) and S-licarbazepine (S-Lic; 300  $\mu\text{M}$ ; red squares). (C) Rundown of  $\text{Na}^+$   
586 current in HEK- $\text{Na}_v1.5$  cells in PSS (black circles) and ESL (300  $\mu\text{M}$ ; red squares). (D) Rundown of  
587  $\text{Na}^+$  current in HEK- $\text{Na}_v1.5$  cells in PSS (black circles) and S-Lic (300  $\mu\text{M}$ ; red squares). Currents  
588 were elicited by 50 Hz pulse trains to 0 mV, applied from a holding potential of -120 mV, normalised  
589 to the current evoked by the first pulse plotted as a function of the pulse number. Data are fitted with  
590 single exponential functions. Results are mean  $\pm$  SEM ( $n = 7-10$ ).

591 **Figure 7.** Effect of eslicarbazepine acetate and S-licarbazepine on recovery from inactivation. (A)  
592 Recovery from inactivation in MDA-MB-231 cells in physiological saline solution (PSS; black  
593 circles) and in eslicarbazepine acetate (ESL; 300  $\mu\text{M}$ ; red squares). (B) Recovery from inactivation in  
594 HEK- $\text{Na}_v1.5$  cells in PSS (black circles) and ESL (300  $\mu\text{M}$ ; red squares). (C) Recovery from  
595 inactivation in MDA-MB-231 cells in PSS (black circles) and S-licarbazepine (S-Lic; 300  $\mu\text{M}$ ; red  
596 squares). (D) Recovery from inactivation in HEK- $\text{Na}_v1.5$  cells in PSS (black circles) and S-Lic (300  
597  $\mu\text{M}$ ; red squares). The fraction recovered ( $I_t/I_c$ ) was determined by a 25 ms pulse to 0 mV ( $I_c$ ),  
598 followed by a recovery pulse to -120 mV for 1-500 ms, and a subsequent 25 ms test pulse to 0 mV  
599 ( $I_t$ ), applied from a holding potential of -120 mV, and plotted as a function of the recovery interval.  
600 Data are fitted with single exponential functions which are statistically different between control and  
601 drug treatments in all cases. Results are mean  $\pm$  SEM ( $n = 7-10$ ).

602 **Figure 8.** Clustal alignment of amino acid sequences of  $\text{Na}_v1.1$ - $\text{Na}_v1.9$  (*SCN1A-SCN11A*). ESL was  
603 proposed previously (51) to interact with the highlighted amino acids in  $\text{Na}_v1.2$ . An alignment of  
604  $\text{Na}_v1.2$  (UniProtKB - Q99250 (SCN2A\_HUMAN)) with  $\text{Na}_v1.1$  (UniProtKB - P35498  
605 (SCN1A\_HUMAN)),  $\text{Na}_v1.3$  (UniProtKB - Q9NY46 (SCN3A\_HUMAN)),  $\text{Na}_v1.4$  (UniProtKB -  
606 P35499 (SCN4A\_HUMAN)),  $\text{Na}_v1.5$  (UniProtKB - Q14524 (SCN5A\_HUMAN))  $\text{Na}_v1.6$   
607 (UniProtKB - Q9UQD0 (SCN8A\_HUMAN)),  $\text{Na}_v1.7$  (UniProtKB - Q15858 (SCN9A\_HUMAN)),  
608  $\text{Na}_v1.8$  (UniProtKB - Q9Y5Y9 (SCN10A\_HUMAN)), and  $\text{Na}_v1.9$  (UniProtKB - Q9UI33  
609 (SCN11A\_HUMAN)) shows that the interacting amino acids highlighted in yellow are conserved  
610 between  $\text{Na}_v1.2$  and  $\text{Na}_v1.5$ , along with most other isoforms. Asterisks indicate conserved residues.  
611 Colon indicates conservation between groups of strongly similar properties - scoring  $> 0.5$  in the  
612 Gonnet PAM 250 matrix. Period indicates conservation between groups of weakly similar properties  
613 - scoring  $\leq 0.5$  in the Gonnet PAM 250 matrix.

614

615 **Table 1.** Effect of eslicarbazepine acetate on Na<sup>+</sup> current characteristics in MDA-MB-231 and HEK-  
616 Na<sub>v</sub>1.5 cells.<sup>1</sup>

<b>A. MDA-MB-231 cells</b>				
<i>Parameter</i>	<i>Control</i>	<i>ESL</i>	<i>P value</i>	<i>N</i>
V <sub>thres</sub> (mV)	-45.7 ± 1.7	-45.0 ± 1.4	0.58	13
V <sub>peak</sub> (mV)	3.1 ± 2.1	-3.9 ± 2.7	0.056	13
Activation V <sup>1/2</sup> (mV)	-19.3 ± 1.4	-22.0 ± 1.5	0.095	12
Activation k (mV)	10.6 ± 0.7	9.3 ± 0.8	0.076	12
Inactivation V <sup>1/2</sup> (mV)	-80.6 ± 0.7	-86.7 ± 1.2	<0.001	13
Inactivation k (mV)	-4.8 ± 0.4	-7.4 ± 1.7	0.139	13
Peak current density at -10 mV (pA/pF)	-14.8 ± 3.9	-8.0 ± 2.5	<0.001	13
Persistent current density at -10 mV (pA/pF)	-0.15 ± 0.05	-0.02 ± 0.07	0.13	12
T <sub>p</sub> at -10 mV (ms)	2.1 ± 0.2	1.9 ± 0.2	<0.01	13
τ <sub>f</sub> at -10 mV (ms)	1.3 ± 0.1	1.3 ± 0.2	0.954	13
τ <sub>s</sub> at -10 mV (ms)	10.0 ± 2.3	6.9 ± 2.0	0.289	13
τ <sub>r</sub> (ms)	6.0 ± 0.5	8.7 ± 0.7	<0.05	10
<b>B. HEK-Na<sub>v</sub>1.5 cells</b>				
<i>Parameter</i>	<i>Control</i>	<i>ESL</i>	<i>P value</i>	<i>N</i>
V <sub>thres</sub> (mV)	-55.0 ± 1.7	-54.0 ± 2.2	0.758	10
V <sub>peak</sub> (mV)	-26.0 ± 2.2	-24.0 ± 4.3	0.591	10
Activation V <sup>1/2</sup> (mV)	-39.4 ± 1.3	-44.2 ± 1.8	<0.05	10
Activation k (mV)	5.3 ± 1.3	3.8 ± 0.7	0.361	10
Inactivation V <sup>1/2</sup> (mV)	-78.2 ± 2.5	-88.3 ± 2.7	<0.001	10
Inactivation k (mV)	-6.9 ± 0.4	-9.8 ± 0.7	<0.001	10
Peak current density at -10 mV (pA/pF)	-154.4 ± 24.0	-33.1 ± 4.7	<0.001	12
Persistent current density at -10 mV (pA/pF)	-0.61 ± 0.15	-0.12 ± 0.05	<0.01	12
T <sub>p</sub> at -10 mV (ms)	1.4 ± 0.2	1.9 ± 0.2	<0.001	14
τ <sub>f</sub> at -10 mV (ms)	0.9 ± 0.1	1.2 ± 0.1	<0.001	12
τ <sub>s</sub> at -10 mV (ms)	6.6 ± 0.8	20.8 ± 8.5	0.128	12
τ <sub>r</sub> (ms)	4.5 ± 0.4	7.1 ± 0.6	<0.001	10

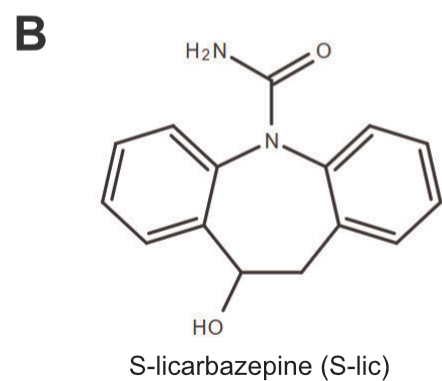
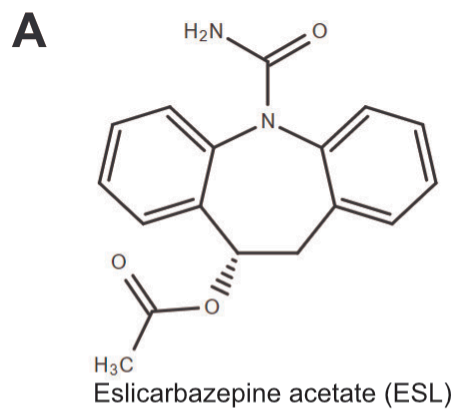
617 <sup>1</sup>ESL: eslicarbazepine acetate (300 μM); V<sub>thres</sub>: threshold voltage for activation; V<sub>peak</sub>: voltage at  
618 which current was maximal; V<sup>1/2</sup>: half (in)activation voltage; k: slope factor for (in)activation; T<sub>p</sub>:  
619 time to peak current; τ<sub>f</sub>: fast time constant of inactivation; τ<sub>s</sub>: slow time constant of inactivation; τ<sub>r</sub>:  
620 time constant of recovery from inactivation. The holding potential was -120 mV. Results are mean ±  
621 SEM. Statistical comparisons were made with paired t-tests.



622 **Table 2.** Effect of S-licarbazepine on Na<sup>+</sup> current characteristics in MDA-MB-231 and HEK-Na<sub>v</sub>1.5  
623 cells.<sup>1</sup>

<b>A. MDA-MB-231 cells</b>				
<i>Parameter</i>	<i>Control</i>	<i>S-Lic</i>	<i>P value</i>	<i>N</i>
V <sub>thres</sub> (mV)	-34.4 ± 2.0	-35.7 ± 2.0	0.603	7
V <sub>peak</sub> (mV)	11.43 ± 4.4	10.0 ± 4.9	0.818	7
Activation V <sub>1/2</sub> (mV)	-12.9 ± 1.3	-13.7 ± 1.4	0.371	7
Activation k (mV)	11.0 ± 0.5	11.9 ± 0.8	0.520	7
Inactivation V <sub>1/2</sub> (mV)	-71.8 ± 2.5	-76.8 ± 2.2	<0.05	7
Inactivation k (mV)	-6.8 ± 0.9	-6.0 ± 1.2	0.302	7
Peak current density at -10 mV (pA/pF)	-12.0 ± 3.1	-6.9 ± 2.5	<0.001	9
Persistent current density at -10 mV (pA/pF)	-1.3 ± 0.4	-0.6 ± 0.2	<0.05	9
T <sub>p</sub> at -10 mV (ms)	4.5 ± 0.4	5.1 ± 0.7	0.103	9
τ <sub>f</sub> at -10 mV (ms)	3.8 ± 1.1	3.2 ± 0.4	0.553	7
τ <sub>s</sub> at -10 mV (ms)	25.7 ± 7.0	27.1 ± 12.0	0.920	7
τ <sub>r</sub> (ms)	6.8 ± 0.4	13.5 ± 1.0	<0.01	7
<b>B. HEK-Na<sub>v</sub>1.5 cells</b>				
<i>Parameter</i>	<i>Control</i>	<i>S-Lic</i>	<i>P value</i>	<i>N</i>
V <sub>thres</sub> (mV)	-50.0 ± 1.9	-51.3 ± 3.5	0.598	9
V <sub>peak</sub> (mV)	-18.0 ± 4.2	-30.0 ± 5.6	<0.001	9
Activation V <sub>1/2</sub> (mV)	-32.8 ± 3.1	-40.5 ± 3.4	<0.01	9
Activation k (mV)	5.9 ± 0.9	4.5 ± 1.1	<0.05	9
Inactivation V <sub>1/2</sub> (mV)	-75.9 ± 2.6	-79.3 ± 4.1	0.116	9
Inactivation k (mV)	-6.5 ± 0.4	-8.1 ± 0.5	<0.05	9
Peak current density at -10 mV (pA/pF)	-140.9 ± 26.8	-77.2 ± 17.0	<0.001	13
Persistent current density at -10 mV (pA/pF)	-0.9 ± 0.2	-0.5 ± 0.2	<0.05	11
T <sub>p</sub> at -10 mV (ms)	1.8 ± 0.5	2.3 ± 0.6	<0.01	13
τ <sub>f</sub> at -10 mV (ms)	1.0 ± 0.04	1.3 ± 0.06	<0.001	11
τ <sub>s</sub> at -10 mV (ms)	6.3 ± 0.5	7.3 ± 0.5	<0.05	11
τ <sub>r</sub> (ms)	5.7 ± 0.7	8.0 ± 1.2	<0.01	10

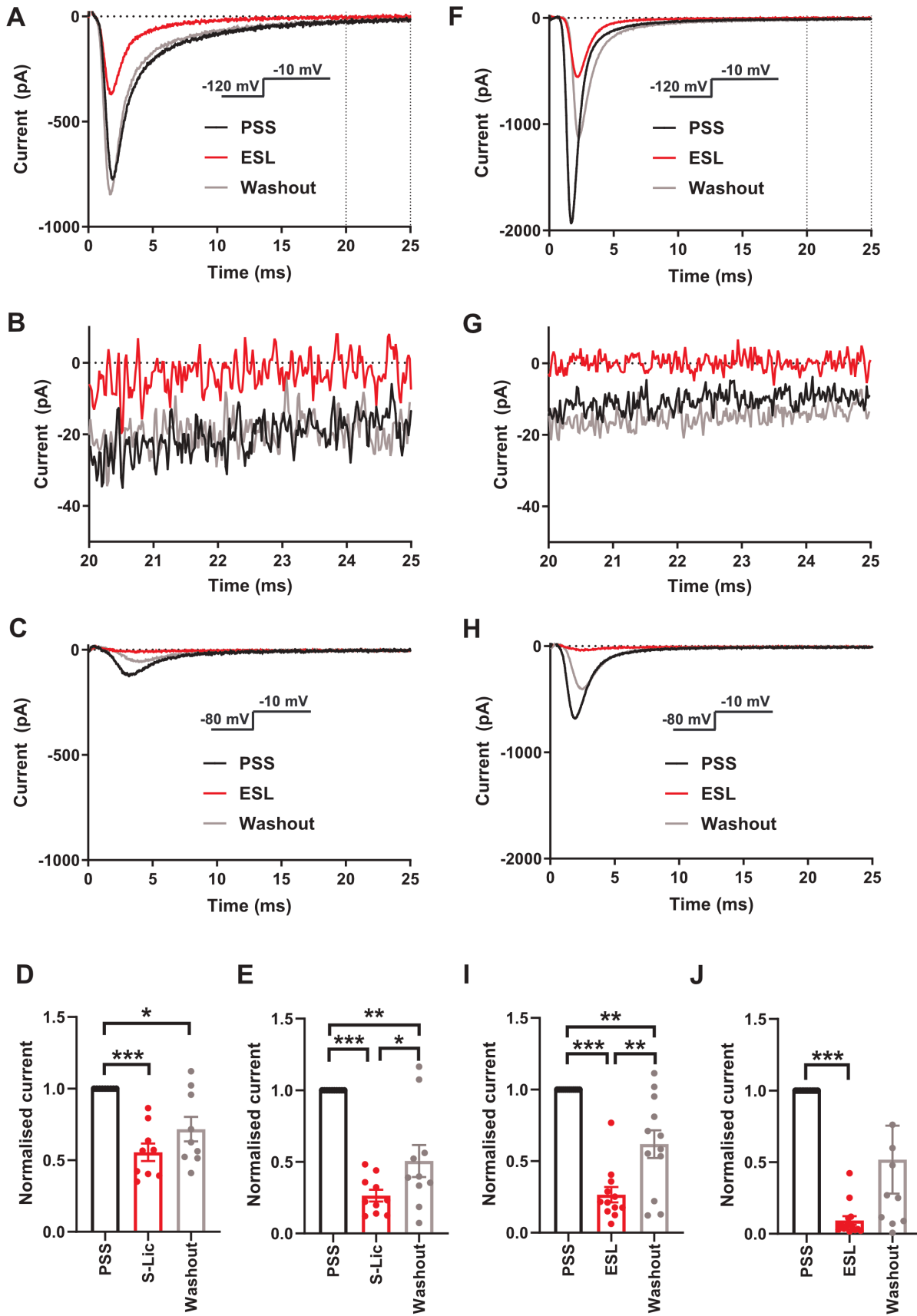
624 <sup>1</sup>S-Lic: S-licarbazepine (300 μM); V<sub>thres</sub>: threshold voltage for activation; V<sub>peak</sub>: voltage at which  
625 current was maximal; V<sub>1/2</sub>: half (in)activation voltage; k: slope factor for (in)activation; T<sub>p</sub>: time to  
626 peak current; τ<sub>f</sub>: fast time constant of inactivation; τ<sub>s</sub>: slow time constant of inactivation; τ<sub>r</sub>: time  
627 constant of recovery from inactivation. The holding potential was -120 mV. Results are mean ± SEM.  
628 Statistical comparisons were made with paired t-tests.



629

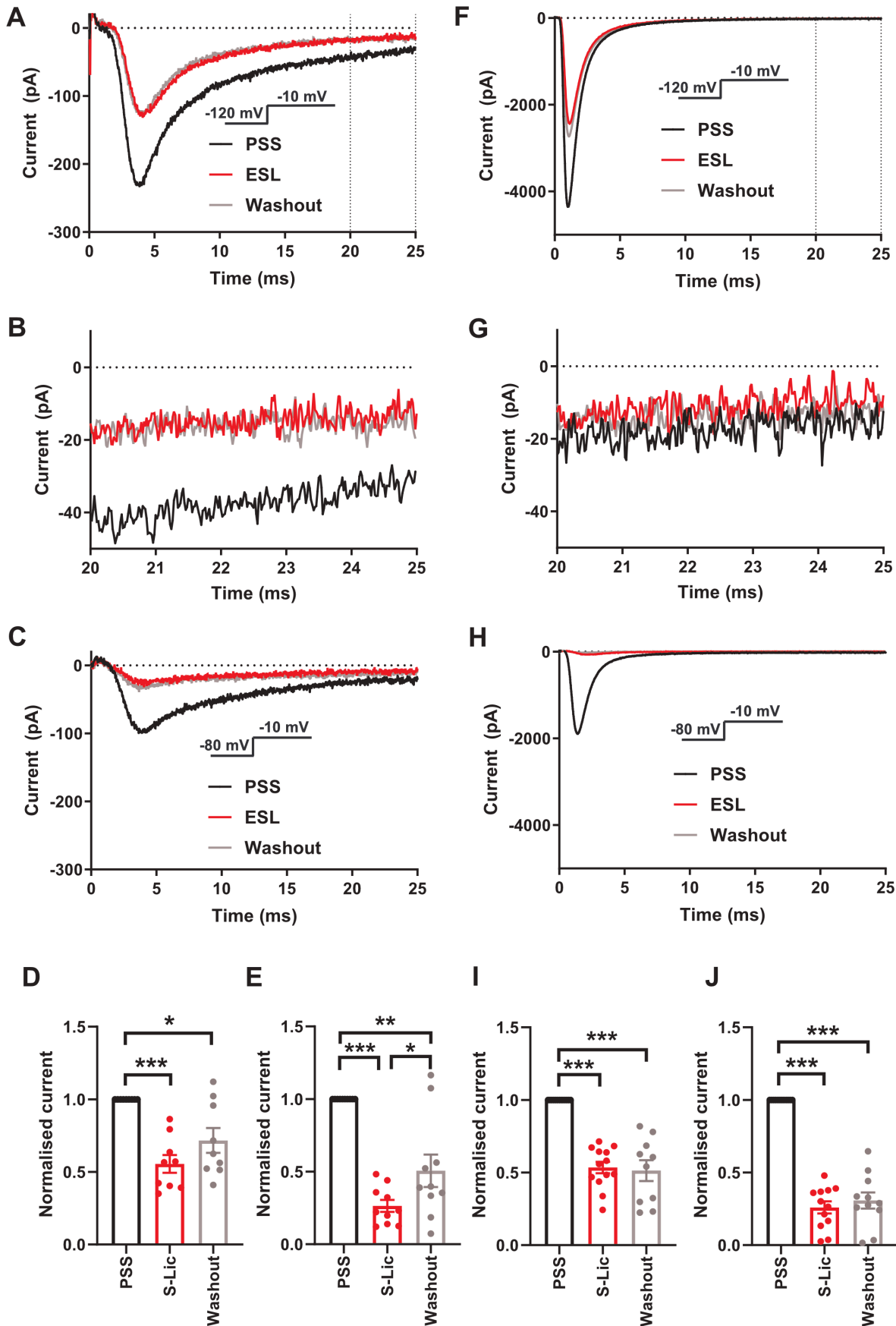
630 Figure 1

631



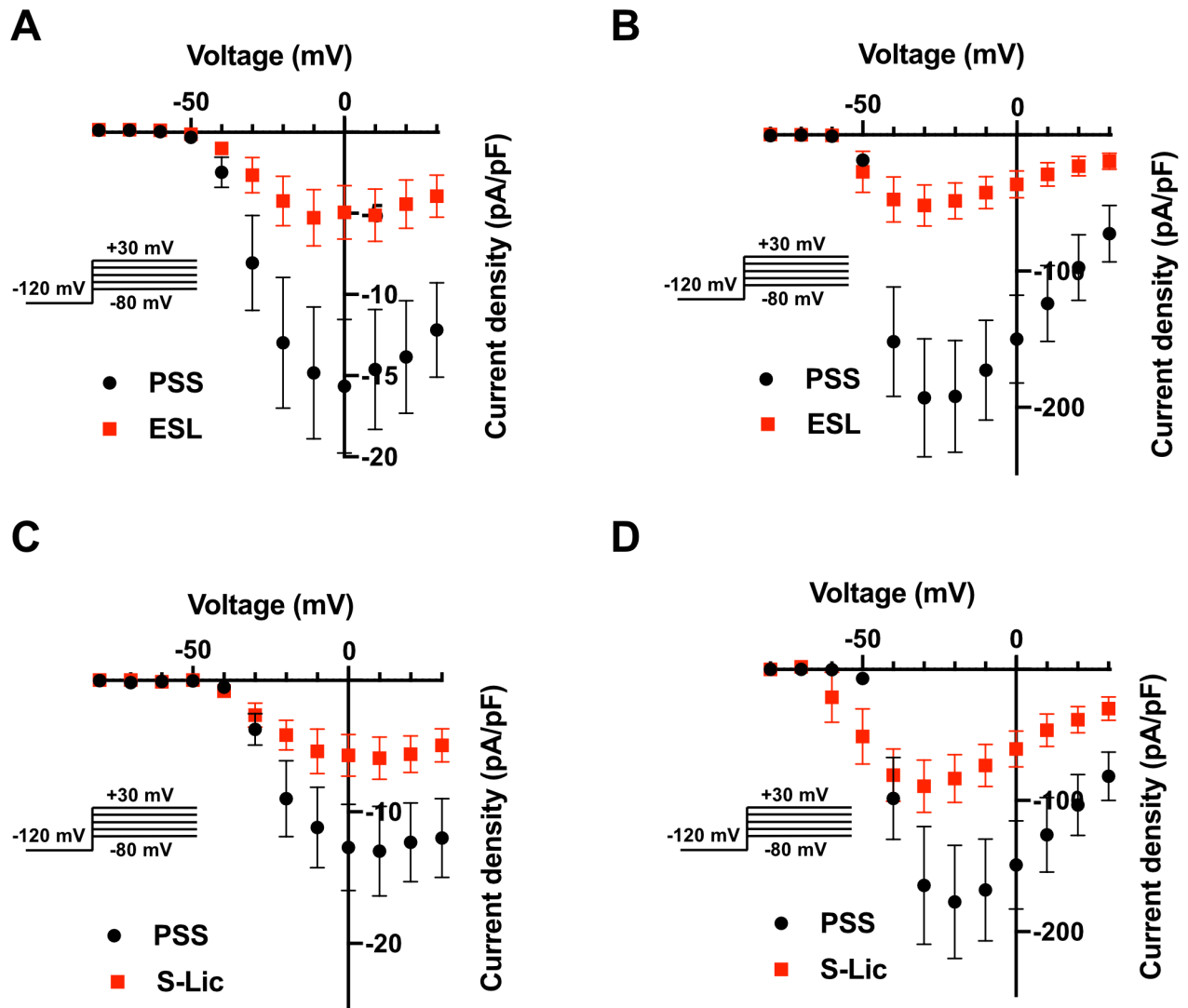
632

633 Figure 2



634

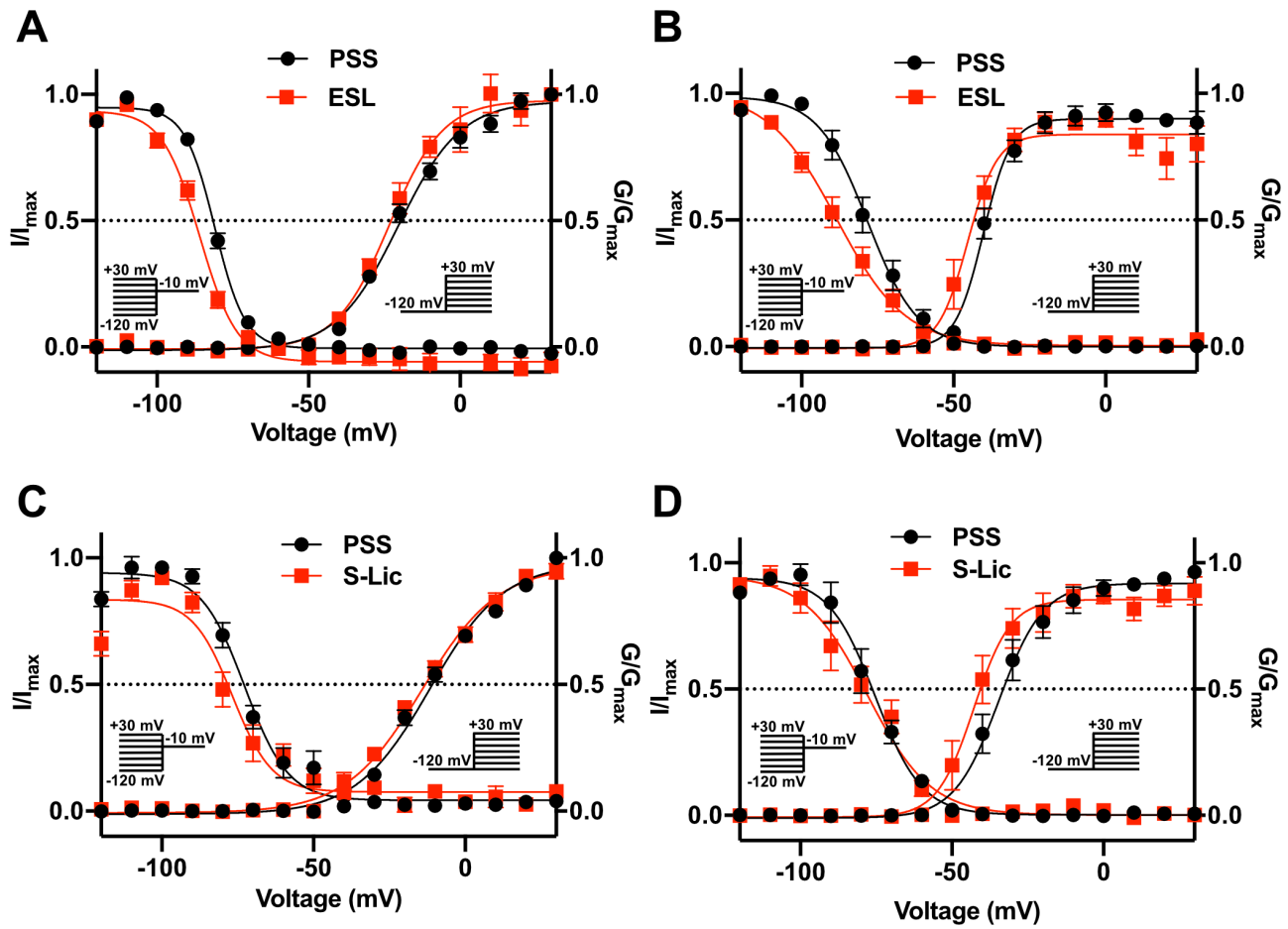
635 Figure 3



636

637 Figure 4

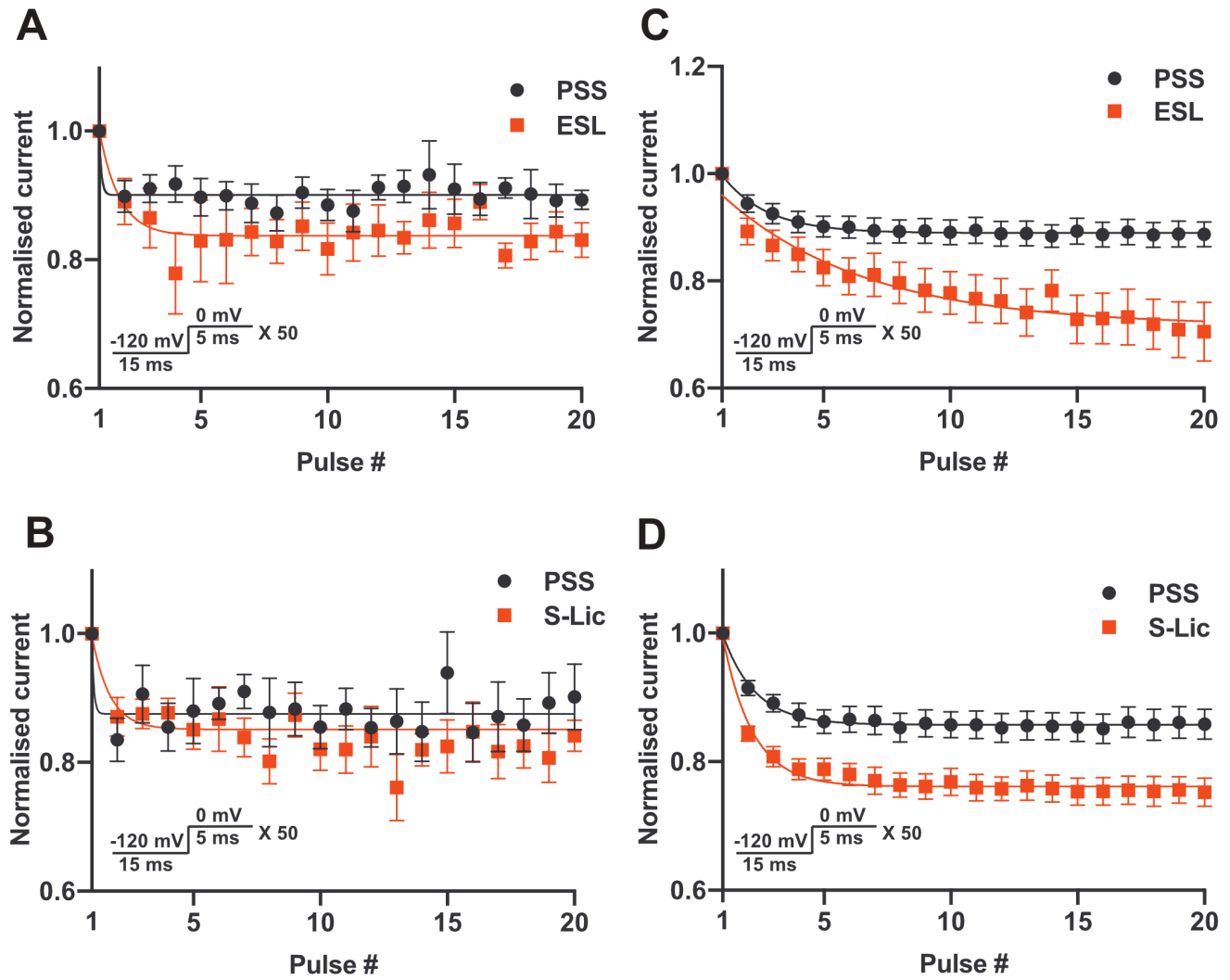
638



639

640 Figure 5

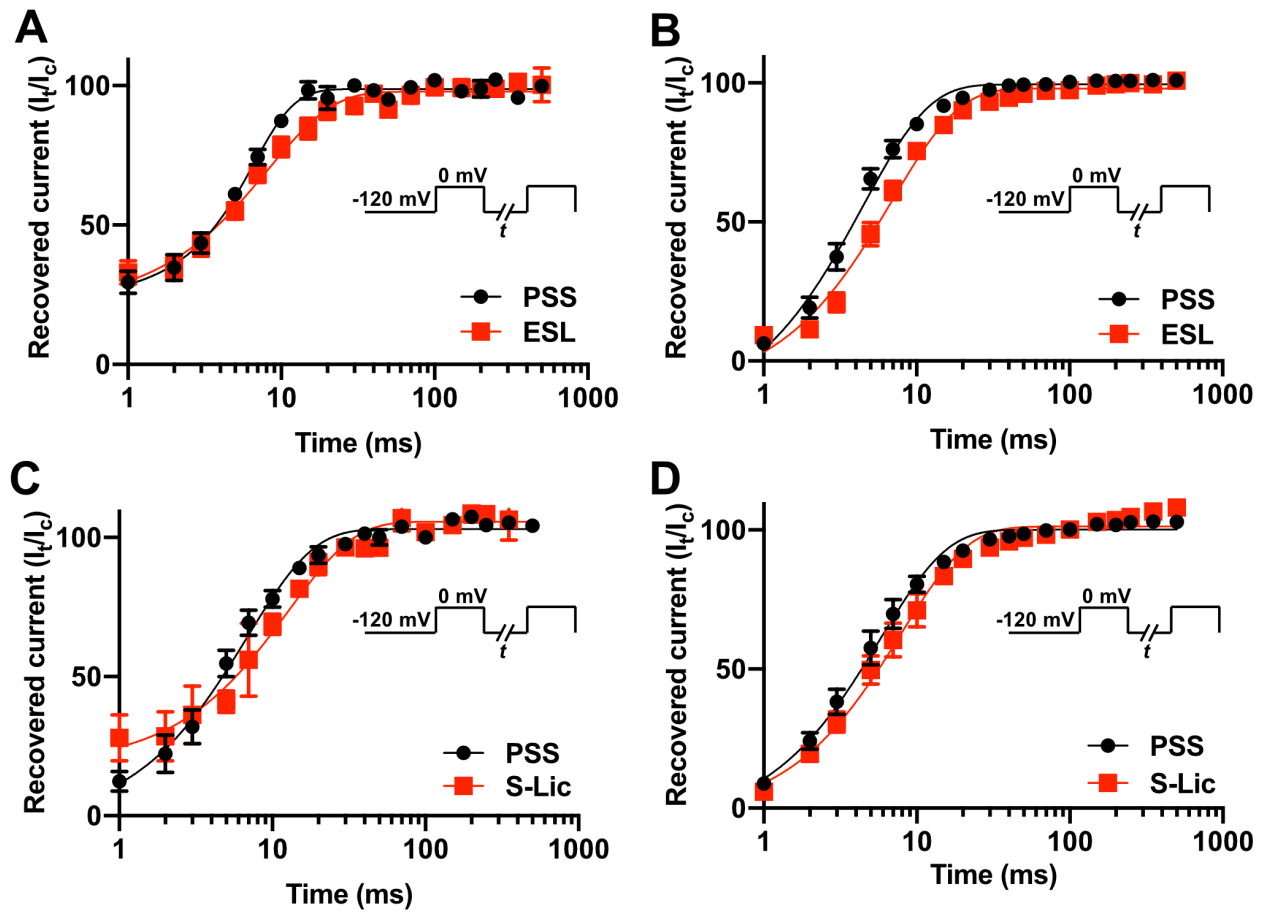
641



642

643 Figure 6

644



645

646 Figure 7

647



SCN1A	I L E N F S V A T E E S A E P L S E D D F E M F Y E V W E K F D P D A T Q F M E F E K L S Q F A A A L E P P L N L P Q P	1844
SCN2A	I L E N F S V A T E E S A E P L S E D D F E M F Y E V W E K F D P D A T Q F I E F A K L S D F A D A L D P P L L I A K P	1834
SCN3A	I L E N F S V A T E E S A E P L S E D D F E M F Y E V W E K F D P D A T Q F I E F S K L S D F A A A L D P P L L I A K P	1829
SCN4A	I L E N F N V A T E E S S E P L G E D D F E M F Y E T W E K F D P D A T Q F I A Y S R L S D F V D T L Q E P L R I A K P	1656
SCN5A	I L E N F S V A T E E S T E P L S E D D F D M F Y E I W E K F D P E A T Q F I E Y S V L S D F A D A L S E P L R I A K P	1830
SCN8A	I L E N F S V A T E E S A D P L S E D D F E T F Y E I W E K F D P D A T Q F I E Y C K L A D F A D A L E H P L R V P K P	1824
SCN9A	I L E N F S V A T E E S T E P L S E D D F E M F Y E V W E K F D P D A T Q F I E F S K L S D F A A A L D P P L L I A K P	1818
SCN10A	I L E N F N V A T E E S T E P L S E D D F D M F Y E T W E K F D P E A T Q F I T F S A L S D F A D T L S G P L R I P K P	1780
SCN11A	I L E N F N T A T E E S E D P L G E D D F D I F Y E V W E K F D P E A T Q F I K Y S A L S D F A D A L P E P L R V A K P	1662
	*****..***** :**.*:**: *** *****:****: : *::*. :* ** : :*	
SCN1A	N K L Q L I A M D L P M V S G D R I H C L D I L F A F T K R V L G E S G E M D A L R I Q M E E R F M A S N P S K V S Y Q	1904
SCN2A	N K V Q L I A M D L P M V S G D R I H C L D I L F A F T K R V L G E S G E M D A L R I Q M E E R F M A S N P S K V S Y E	1894
SCN3A	N K V Q L I A M D L P M V S G D R I H C L D I L F A F T K R V L G E S G E M D A L R I Q M E D R F M A S N P S K V S Y E	1889
SCN4A	N K I K L I T L D L P M V P G D K I H C L D I L F A L T K E V L G D S G E M D A L K Q T M E E K F M A A N P S K V S Y E	1716
SCN5A	N Q I S L I N M D L P M V S G D R I H C M D I L F A F T K R V L G E S G E M D A L K I Q M E E K F M A A N P S K I S Y E	1890
SCN8A	N T I E L I A M D L P M V S G D R I H C L D I L F A F T K R V L G D S G E L D I L R Q Q M E E R F V A S N P S K V S Y E	1884
SCN9A	N K V Q L I A M D L P M V S G D R I H C L D I L F A F T K R V L G E S G E M D S L R S Q M E E R F M S A N P S K V S Y E	1878
SCN10A	N R N I L I Q M D L P L V P G D K I H C L D I L F A F T K N V L G E S G E L D S L K A N M E E K F M A T N L S K S S Y E	1840
SCN11A	N K Y Q F L V M D L P M V S E D R L H C M D I L F A F T A R V L G G S D G L D S M K A M M E E K F M E A N P L K K L Y E	1722
	* : : ***** * *::***:*****:* .*** *. :* :: *::*: : * * * :	

648

649 Figure 8